The authors sincerely thank the Reviewer for the careful review and thoughtful comments, which are very helpful in improving our manuscript. Comments from the Reviewer are reproduced in black font. Our point-by-point responses to the comments raised by the Reviewer are indicated in blue font below and the revised text in the manuscript is shown in red.

Reviewer: 1

The manuscript by Yang et al. describes a set of laboratory measurements, in which they investigated SO2 effects on the formation and chemical composition of particles from anthropogenic volatile organic compound ozonolysis. Various monomeric and dimeric products with C, H, and O atoms were observed under SO2-free conditions. The authors found that SO2 presence can induce the formation of sulfur-containing compounds. They suggested that the observed sulfur-containing compounds have stronger ability for particle formation than corresponding precursors, leading to an enhancement of particle formation. Structures and reasonable formation mechanisms of these sulfur-containing compounds were also proposed. Overall, the experimental design, results, and discussion of this manuscript are presented in a logical sequence that is easy to follow and understand. The paper provides new and valuable results for our understanding of the details of SO2 roles in aerosol formation, and also guidance and inspiration for the community that reads ACP. Therefore, I would recommend the publication of this work if the author consider the minor comments below.

Specific comments:

The authors did a great job of explaining the reasons why their study would be of importance and interest. However, there is just brief text regarding the influences of SO2 on aerosol chemistry. Some recent literatures should be considered.

Deng, P. S. J. Lakey, Y. Wang, P. Li, J. Xu, H. Pang, J. Liu, X. Xu, X. Li, X. Wang, Y. Zhang, M. Shiraiwa and S. Gligorovski, Daytime SO2 chemistry on ubiquitous urban surfaces as a source of organic sulfur compounds in ambient air, Sci. Adv., 2022, 8, eabq6830.

Wang, T. Liu, J. Jang, J. P. D. Abbatt and A. W. H. Chan, Heterogeneous interactions between SO2 and organic peroxides in submicron aerosol, Atmos. Chem. Phys., 2021, 21, 6647-6661.

Response:

The literatures recommended by the Reviewer have been cited in the revised manuscript.

The following text was also added in the Introduction section to complement the influences of SO_2 on aerosol composition.

Page 2, Line 39:

Recently, the impacts of inorganic gases on aerosol chemistry have received significant attention (Deng et al., 2022).

Page 2, Line 51:

For instance, under humid condition, the reactive uptake of SO_2 onto organic aerosols was obvious and reactions of SO_2 with organic peroxides could contribute to organosulfate (OS) formation (Wang et al., 2021a; Ye et al., 2018). H_2SO_4 originated from sCI-induced oxidation of SO_2 is also linked to OS production (Stangl et al., 2019).

P4, L92. The authors mentioned that cyclohexane was injected into the chamber to scavenge OH radical. It is also worth mentioning how did the authors determine that OH had been successfully scavenged.

Response:

Aerosol yield from OH oxidation of cyclohexane is relatively low, and cyclohexane hardly reacts with O_3. Therefore, cyclohexane is commonly employed to isolate SOA formation from the additional impacts of OH formed in the gas-phase reaction of O_3 with alkenes (Bracco et al., 2019; Carlsson et al., 2012; Sato et al., 2013; Ng et al., 2006).

In this work, cyclohexane was introduced into the chamber at sufficient concentration (~130 ppm) so that more than 98% of OH generated during the ozonolysis of cyclooctene were scavenged. Control experiments were also carried out, and the corresponding results showed that the presence of cyclohexane could lead to the significant decrease in particle volume concentration (Fig. R1).

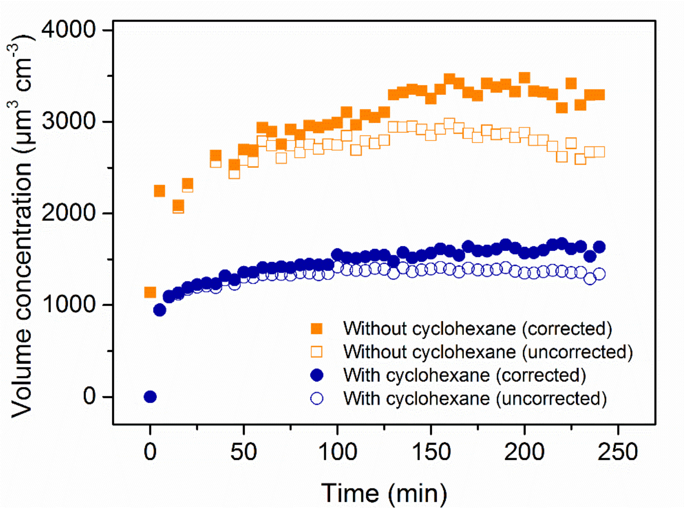

Figure R1. Particle volume concentration as a function of time during the ozonolysis of cyclooctene with and without cyclohexane addition.

For clarification, the following text was inserted in the experimental method section, and Fig. R1 was added in the revised supplement.

Page 4, Line 95:

Cyclohexane (99.5%, Aladdin) was injected in excess (~130 ppm) into the chamber so that more than 98% of OH generated during the ozonolysis of cyclooctene were scavenged. Control experiments showed that the presence of cyclohexane could lead to the significant decrease in particle volume concentration (Fig. S1).

P5, L118 and L128. Particle production experiments were carried out as batch mode experiments. Therefore, the chemical reaction systems were evolving during the ozonolysis of anthropogenic volatile compound. During which reaction period of the experiments did the authors collect aerosol particles? Please indicate this information.

Response:

Aerosol particles were collected 300 min after the reaction initiation. For clarification, the following sentence was added in the method section.

Page 5, Line 115:

The particle formation experiments proceeded for 300 min before the collection of aerosol particles.

P6, L130. It should be also stated clear how the extraction was done (i.e., whole filter or punches? device?)

Response:

The original sentence has been revised to show more details about the extraction method.

Page 6, Line 139:

The whole sample filters were extracted twice into 5 mL of methanol (Optima® LC-MS grade, Fisher Scientific) by ice sonication (KQ5200E, Kunshan Ultrasonic Instruments, China) for 20 min.

P7, L162–167. Perhaps it is better for the understanding of readers to include some relevant citations.

Response:

The KMD method has been widely applied for the analysis of mass spectra of organic aerosols. For clarification, the following sentence and references were added in the revised manuscript.

Page 7, Line 178:

The KMD value is same for homologous species that differ from each other only by their base units.

Kenseth, C. M., Hafeman, N. J., Huang, Y., Dalleska, N. F., Stoltz, B. M., and Seinfeld, J. H.: Synthesis of Carboxylic Acid and Dimer Ester Surrogates to Constrain the Abundance and Distribution of Molecular Products in alpha-Pinene and beta-Pinene Secondary Organic Aerosol, Environ. Sci. Technol., 54, 12829-12839, 10.1021/acs.est.0c01566, 2020.

Kundu, S., Fisseha, R., Putman, A. L., Rahn, T. A., and Mazzoleni, L. R.: Molecular formula composition of β-caryophyllene ozonolysis SOA formed in humid and dry

conditions, Atmos. Environ., 154, 70-81, 10.1016/j.atmosenv.2016.12.031, 2017.

P7, L168. Full equation from Li et al. (2016) should be given.

Response:

The following formulation has been updated in the revised manuscript.

$$\log_{10} C_i^{\mathrm{o}} = (n_{\mathrm{C}}^{0}\text{-}n_{\mathrm{C}}^{i})b_{\mathrm{C}}\text{-}n_{\mathrm{O}}^{i}b_{\mathrm{O}}\text{-}2\frac{n_{\mathrm{C}}^{i}n_{\mathrm{O}}^{i}}{n_{\mathrm{C}}^{i}+n_{\mathrm{O}}^{i}}b_{\mathrm{CO}}\text{-}n_{\mathrm{N}}^{i}b_{\mathrm{N}}\text{-}n_{\mathrm{S}}^{i}b_{\mathrm{S}}$$

P9, L225. From Fig. S2, the volume concentration of aerosol particles reached its maximum within 240 min. So, what is the definition of the initial stage of particle production experiment?

Response:

Once O_3 was introduced into the reactor, cyclooctene began to be oxidized and aerosol particles were produced rapidly. Based on the initial concentrations of O_3 (~800 ppb) and cyclooctene (~200 ppb) as well as the reaction rate constant (4.51×10^{-16} cm^3 molecule^{-1} s^{-1}), the reaction of cyclooctene with O_3 could be completed within several minutes. GC-FID measurements also indicated that cyclooctene was completely consumed within 10 minutes after the ozonolysis was initiated. When cyclooctene was depleted, aerosol particle mass increased slowly. Therefore, the initial stage of particle formation in this work was defined as the time (~10 min) from reaction initiation to the complete consumption of cyclooctene.

Now, the definition of the initial stage of particle production experiment is provided in the revised manuscript.

Page 10, line 242:

Once O_3 was introduced into the reactor, aerosol particles were produced rapidly. After cyclooctene was depleted, the aerosol particle mass increased slowly. The initial stage of particle formation was then defined as the time from reaction initiation to the complete consumption of cyclooctene (~10 min).

The authors mentioned that the enhancement of aerosol particles was mainly due to the formation of inorganic and organic sulfates. Although wall losses of organic vapors may be negligible as the author discussed, previous studies suggest that increased particle surface area by SO2 may cause the increase in particle volume concentration. Would this be a possible clarification?

Response:

As suggested by the Reviewer, condensation of organic vapors onto aerosol particles can compete with wall losses of organic vapors. To better investigate the roles of SO_2 via increasing particle surface in promoting particle formation, we calculated the timescales associated with gas-particle partitioning equilibrium ($\tau_{g\text{-}p}$, s) and gas-wall equilibrium ($\tau_{g\text{-}w}$, s) based on the method of Zhang et al. (2014). More details about this method are shown below.

(a) Gas-wall equilibrium. The wall-loss process of gas-phase products is generally taken into account to be first-order and the first-order wall-loss coefficient of gas-phase products, k_w (s^{-1}), can be calculated as

$$k_w = \frac{A}{V} \times \frac{0.25\alpha_w \bar{c}}{1.0 + \frac{\pi}{2} \times \frac{\alpha_w \bar{c}}{4(k_e D_{gas})^{0.5}}} \tag{R1}$$

where A/V (5.55 m^{-1}) is the surface to volume ratio of Teflon reactor; α_w is the mass accommodation coefficient of gas-phase products onto the inner wall and an α_w value of 10^{-5} was employed (Matsunaga and Ziemann, 2010; Zhang et al., 2014); $\bar{c}$ ($m\ s^{-1}$) is the molecules' mean thermal speed; k_e (s^{-1}) and D_{gas} ($m^2\ s^{-1}$) are the eddy diffusion coefficient and the molecular diffusivity, respectively. A k_e value of 0.02 s^{-1} was adopted (Mcmurry and Grosjean, 1985). D_{gas} was estimated to be 6×10^{-6} $m^2\ s^{-1}$ (Krechmer et al., 2017; Tang et al., 2015). MW ($g\ mol^{-1}$) is molecular weight of the given gas-phase product. An average molecular weight of 200 $g\ mol^{-1}$ for gas-phase products was used to estimate the influence of vapor wall loss (Sarrafzadeh et al., 2016).

The mean thermal speed could be determined according to the following equation:

$$\bar{c} = \sqrt{\frac{8RT}{\pi MW}} \tag{R2}$$

where R (8.314 J mol^{-1} K^{-1}) and T (K) are the ideal gas constant and experimental temperature, respectively.

The time required to approach gas-wall equilibrium ($\tau_{\text{g-w}}$, s) can be calculated as:

$$\tau_{\text{g-w}} = \frac{1}{k_w} \tag{R3}$$

(b) Gas-particle equilibrium. The time associated with approaching gas-particle equilibrium ($\tau_{\text{g-p}}$, s) can be determined using the following equation:

$$\tau_{g\text{-}p} = \frac{1}{2\pi N_p \overline{D_p}\, D_{gas} \overline{F_{FS}}} \tag{R4}$$

where N_p (# m^{-3}) and $\overline{D_p}$ (m) are the number concentration and mean diameter of aerosol particles, respectively; D_{gas} (m^2 s^{-1}) is the molecular diffusivity. $\overline{F_{FS}}$ is the Fuchs-Sutugin correction and it is equal to:

$$\overline{F_{FS}} = \frac{0.75\alpha_p(1+k_n)}{k_n^2 + k_n + 0.283k_n\alpha_p + 0.75\alpha_p} \tag{R5}$$

where α_p is the mass accommodation coefficient of gas-phase products onto aerosol particles. An α_p value of 0.7 was adopted (Krechmer et al., 2017). K_n is the Knudsen number, which can be calculated as:

$$k_n = \frac{2\lambda}{D_p} \tag{R6}$$

The gas mean free path (λ, nm) of gas-phase product is defined as:

$$\lambda = \frac{3D_{gas}}{\bar{c}} \tag{R7}$$

The value of $\tau_{\text{g-w}}$ was determined to be around 20.4 ± 0.01 min. The estimated $\tau_{\text{g-p}}$ value decreased from 0.13 ± 0.01 to 0.07 ± 0.01 min when SO_2 concentrations increased from 0 to 129 ppb. Gas-particle partitioning could dominate the wall deposition of gas-phase products for particle number concentrations in our chamber experiments. Therefore, the roles of SO_2 via increasing particle surface in promoting particle formation may be negligible.

For clarification, the following details about the calculation of gas-particle partitioning equilibrium and gas-wall equilibrium were inserted into the revised supplement.

S1. Estimation of wall losses of organic vapors

(a) Gas-wall equilibrium. The wall-loss process of gas-phase products is generally taken into account to be first-order and the first-order wall-loss coefficient of gas-phase products, k_w (s^{-1}), can be calculated as

$$k_w = \frac{A}{V} \times \frac{0.25\alpha_w\bar{c}}{1.0 + \frac{\pi}{2} \times \frac{\alpha_w\bar{c}}{4(k_e D_{gas})^{0.5}}} \qquad \text{(S1)}$$

where A/V (5.55 m^{-1}) is the surface to volume ratio of Teflon reactor; α_w is the mass accommodation coefficient of gas-phase products onto the inner wall and an α_w value of 10^{-5} was employed (Matsunaga and Ziemann, 2010; Zhang et al., 2014); $\bar{c}$ ($m\ s^{-1}$) is the molecules' mean thermal speed; k_e (s^{-1}) and D_{gas} ($m^2\ s^{-1}$) are the eddy diffusion coefficient and the molecular diffusivity, respectively. A k_e value of 0.02 s^{-1} was adopted (Mcmurry and Grosjean, 1985). D_{gas} was estimated to be 6×10^{-6} $m^2\ s^{-1}$ (Krechmer et al., 2017; Tang et al., 2015). MW ($g\ mol^{-1}$) is molecular weight of the given gas-phase product. An average molecular weight of 200 $g\ mol^{-1}$ for gas-phase products was used to estimate the influence of vapor wall loss (Sarrafzadeh et al., 2016).

The mean thermal speed could be determined according to the following equation:

$$\bar{c} = \sqrt{\frac{8RT}{\pi MW}} \qquad \text{(S2)}$$

where R (8.314 $J\ mol^{-1}\ K^{-1}$) and T (K) are the ideal gas constant and experimental temperature, respectively.

The time required to approach gas-wall equilibrium ($\tau_{g\text{-}w}$, s) can be calculated as:

$$\tau_{g\text{-}w} = \frac{1}{k_w} \qquad \text{(S3)}$$

(b) Gas-particle equilibrium. The time associated with approaching gas-particle equilibrium ($\tau_{g\text{-}p}$, s) can be determined using the following equation:

$$\tau_{g\text{-}p} = \frac{1}{2\pi N_p \overline{D_p}\, D_{gas} \overline{F_{FS}}} \qquad \text{(S4)}$$

where N_p (# m^{-3}) and $\overline{D_p}$ (m) are the number concentration and mean diameter of aerosol particles, respectively; D_{gas} (m^2 s^{-1}) is the molecular diffusivity. $\overline{F_{FS}}$ is the Fuchs-Sutugin correction and it is equal to:

$$\overline{F_{FS}} = \frac{0.75\alpha_p(1+k_n)}{k_n^2 + k_n + 0.283k_n\alpha_p + 0.75\alpha_p} \tag{S5}$$

where α_p is the mass accommodation coefficient of gas-phase products onto aerosol particles. An α_p value of 0.7 was adopted (Krechmer et al., 2017). K_n is the Knudsen number, which can be calculated as:

$$k_n = \frac{2\lambda}{D_p} \tag{S6}$$

The gas mean free path (λ, nm) of gas-phase product is defined as:

$$\lambda = \frac{3D_{gas}}{\bar{c}} \tag{S7}$$

The value of $\tau_{g\text{-}w}$ was determined to be around 20.4 ± 0.01 min. The estimated $\tau_{g\text{-}p}$ value decreased from 0.13 ± 0.01 to 0.07 ± 0.01 min when SO_2 concentrations increased from 0 to 129 ppb. Gas-particle partitioning could dominate the wall deposition of gas-phase products for particle number concentrations in our chamber experiments.

P17, L378. Could you provide some more details about the IR absorption of different functional groups? Perhaps in the Supplement?

Response:

The IR absorption of assigned functional groups are summarized in the following Table, and they have been inserted in the revised supplement.

Table R1. IR absorption of functional groups.

Assignment	**Wavenumber (cm^{-1})**	**References**
H-bonding of OH in alcohol	3600–3200	(Hung et al., 2013)
H-bonding of carboxylic acid	3200–2400	(Sax et al., 2005)
aliphatic CH	3000–2800	(Sax et al., 2005)
C=O in carboxylic acid/ketone/aldehyde/ester	1750–1685	(Hung et al., 2013)
OH of alcohol in-plane deformation vibration	1440–1260	
C-O stretching in primary alcohol	1090–1000	
C-O stretching in secondary alcohol	1150–1075	
C-O stretching in tertiary alcohol	1210–1100	
C-O stretching in carboxylic acid	1320–1210	
C-O stretching in peroxide	1150–1030	
asymmetric SO_2 stretching	1415–1370	(Tammer, 2004)
C-O-C stretching	1050–1010	(Liu et al., 2015)
C-O-C stretching in acetal	1085	(Lal et al., 2012)
symmetric SO_2 stretching	1064	(Lal et al., 2012)
C-O vibration of C-O-S	1050–1030	(Hung et al., 2013)
asymmetric SO stretching	1020–850	(Hung et al., 2013)
C-O-C stretching in ether	950	(Lin et al., 2014)
O-O stretching in peroxide	900–800	(Hung et al., 2013)
asymmetric C-O-S stretching	875	(Tammer, 2004)
symmetric C-O-S stretching	750	

P19, L 396. The Reviewer would recommend the author to present briefly the strengths of ESI-MS in characterizing organosulfate. This may be significant in supporting the production of organosulfate.

Response:

Traditional analytical methods, for example GC-MS techniques, failed to measure organosulfates (Surratt et al., 2007). In contrast, UHPLC-HRMS coupled with ESI has been recognized as a robust and effective method for the analysis of organosulfate in aerosol samples (Riva et al., 2016; Bruggemann et al., 2020; Wang et al., 2021b). Organosulfates could undergo highly efficient ionization to give deprotonated molecular ions in negative ion mode without derivatization. Orbitrap MS with high sensitivity and molecular specificity allows us to accurately assign an amount of mass spectral signals to organosulfates (Eliuk and Makarov, 2015; Bruggemann et al., 2020). Furthermore, unambiguous identification of organosulfates can be achieved based on tandem mass spectrometry analysis because organosulfates could give characteristic fragment ions at *m/z* 80 (SO_3^-), 81 (HSO_3^-), and/or 97 (HSO_4^-).

The following text has been added to enrich the description about ESI-MS in the revised manuscript.

Page 20, Line 415:

OS could undergo highly efficient ionization to give deprotonated molecular ions in negative ion mode. Based on MS/MS analysis, unambiguous identification of OS can be achieved since OSs could give characteristic fragment ions at *m/z* 80 (SO_3^-), 81 (HSO_3^-), and/or 97 (HSO_4^-) in their MS/MS spectra.

P22, Figure 7. The legend "Precursor" is confusing since cyclooctene is also referred to as a precursor in this manuscript. Suggest different legend such as organosulfate precursor or something else.

Response:

Legend has been updated in the revised manuscript as follows:

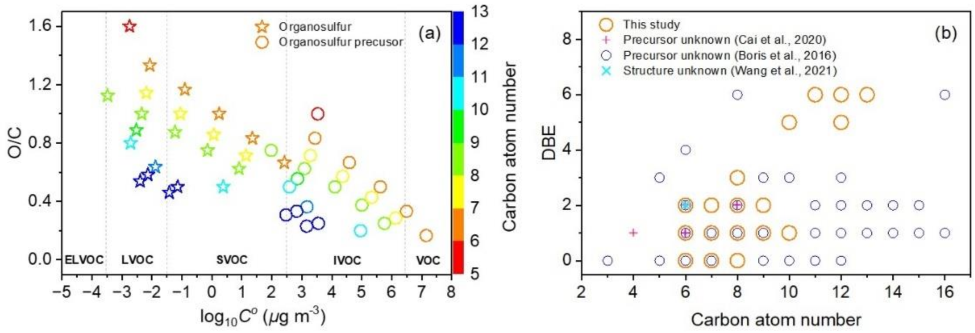

Figure 7. (a) Two dimensional volatility–oxidation space of the identified organosulfurs and their precursors. (b) Carbon atom number distribution of organosulfurs observed in the current work and in the studies of Cai et al. (2020), Boris et al. (2016), and Wang et al. (2021). Detailed formulae of these OSs can be found in Table S3. Organosulfurs from previous studies are of unknown origin or unknown structure.

References

Bracco, L. L. B., Tucceri, M. E., Escalona, A., Diaz-de-Mera, Y., Aranda, A., Rodriguez, A. M., and Rodriguez, D.: New particle formation from the reactions of ozone with indene and styrene, Phys. Chem. Chem. Phys., 21, 11214-11225, 10.1039/c9cp00912d, 2019.

Bruggemann, M., Xu, R., Tilgner, A., Kwong, K. C., Mutzel, A., Poon, H. Y., Otto, T., Schaefer, T., Poulain, L., Chan, M. N., and Herrmann, H.: Organosulfates in Ambient Aerosol: State of Knowledge and Future Research Directions on Formation, Abundance, Fate, and Importance, Environ. Sci. Technol., 54, 3767-3782, 10.1021/acs.est.9b06751, 2020.

Carlsson, P. T., Keunecke, C., Kruger, B. C., Maass, M. C., and Zeuch, T.: Sulfur dioxide oxidation induced mechanistic branching and particle formation during the ozonolysis of β-pinene and 2-butene, Phys. Chem. Chem. Phys., 14, 15637-15640, 10.1039/c2cp42992f, 2012.

Deng, H., Lakey, P. S. J., Wang, Y., Li, P., Xu, J., Pang, H., Liu, J., Xu, X., Li, X., Wang, X., Zhang, Y., Shiraiwa, M., and Gligorovski, S.: Daytime SO_2 chemistry on ubiquitous urban surfaces as a source of organic sulfur compounds in ambient air, Sci. Adv., 8, eabq6830, doi:10.1126/sciadv.abq6830, 2022.

Eliuk, S. and Makarov, A.: Evolution of Orbitrap Mass Spectrometry Instrumentation, Annu Rev Anal Chem (Palo Alto Calif), 8, 61-80, 10.1146/annurev-anchem-071114-040325, 2015.

Hung, H. M., Chen, Y. Q., and Martin, S. T.: Reactive aging of films of secondary organic material studied by infrared spectroscopy, J. Phys. Chem. A, 117, 108-116, 10.1021/jp309470z, 2013.

Krechmer, J. E., Day, D. A., Ziemann, P. J., and Jimenez, J. L.: Direct Measurements of Gas/Particle Partitioning and Mass Accommodation Coefficients in Environmental Chambers, Environ. Sci. Technol., 51, 11867-11875, 10.1021/acs.est.7b02144, 2017.

Lal, V., Khalizov, A. F., Lin, Y., Galvan, M. D., Connell, B. T., and Zhang, R.: Heterogeneous reactions of epoxides in acidic media, J. Phys. Chem. A, 116, 6078-6090, 10.1021/jp2112704, 2012.

Lin, Y. H., Budisulistiorini, H., Chu, K., Siejack, R. A., Zhang, H. F., Riva, M., Zhang, Z. F., Gold, A., Kautzman, K. E., and Surratt, J. D.: Light-Absorbing Oligomer Formation in Secondary Organic Aerosol from Reactive Uptake of Isoprene Epoxydiols, Environ. Sci. Technol., 48, 12012-12021, 10.1021/es503142b, 2014.

Liu, Y., Liggio, J., Staebler, R., and Li, S. M.: Reactive uptake of ammonia to secondary organic aerosols: kinetics of organonitrogen formation, Atmos. Chem. Phys., 15, 13569-13584, 10.5194/acp-15-13569-2015, 2015.

Matsunaga, A. and Ziemann, P. J.: Gas-Wall Partitioning of Organic Compounds in a Teflon Film Chamber and Potential Effects on Reaction Product and Aerosol Yield Measurements, Aerosol Sci. Technol., 44, 881-892, 10.1080/02786826.2010.501044, 2010.

McMurry, P. H. and Grosjean, D.: Gas and aerosol wall losses in Teflon film smog chambers, Environ. Sci. Technol., 19, 1176-1182, 10.1021/es00142a006, 1985.

Ng, N. L., Kroll, J. H., Keywood, M. D., Bahreini, R., Varutbangkul, V., Flagan, R. C., Seinfeld, J. H., Lee, A., and Goldstein, A. H.: Contribution of first- versus second-generation products to secondary organic aerosols formed in the oxidation of biogenic hydrocarbons, Environ. Sci. Technol., 40, 2283-2297, 10.1021/es052269u, 2006.

Riva, M., Barbosa, T. D. S., Lin, Y.-H., Stone, E. A., Gold, A., and Surratt, J. D.: Chemical characterization of organosulfates in secondary organic aerosol derived from the photooxidation of alkanes, Atmos. Chem. Phys., 16, 11001-11018, 10.5194/acp-16-11001-2016, 2016.

Sarrafzadeh, M., Wildt, J., Pullinen, I., Springer, M., Kleist, E., Tillmann, R., Schmitt, S. H., Wu, C., Mentel, T. F., Zhao, D., Hastie, D. R., and Kiendler-Scharr, A.: Impact of NO_x and OH on secondary organic aerosol formation from β-pinene photooxidation, Atmos. Chem. Phys., 16, 11237-11248, 10.5194/acp-16-11237-2016, 2016.

Sato, K., Inomata, S., Xing, J.-H., Imamura, T., Uchida, R., Fukuda, S., Nakagawa, K., Hirokawa, J., Okumura, M., and Tohno, S.: Effect of OH radical scavengers on secondary organic aerosol formation from reactions of isoprene with ozone, Atmos. Environ., 79, 147-154, 10.1016/j.atmosenv.2013.06.036, 2013.

Sax, M., Zenobi, R., Baltensperger, U., and Kalberer, M.: Time resolved infrared spectroscopic analysis of aerosol formed by photo-oxidation of 1,3,5-trimethylbenzene and alpha-pinene, Aerosol Sci. Technol., 39, 822-830, 10.1080/02786820500257859, 2005.

Stangl, C. M., Krasnomowitz, J. M., Apsokardu, M. J., Tiszenkel, L., Ouyang, Q., Lee, S., and Johnston, M. V.: Sulfur dioxide modifies aerosol particle formation and growth by ozonolysis of monoterpenes and isoprene, J. Geophys. Res.-Atmos., 124, 4800-4811, 2019.

Surratt, J. D., Kroll, J. H., Kleindienst, T. E., Edney, E. O., Claeys, M., Sorooshian, A., Ng, N. L., Offenberg, J. H., Lewandowski, M., Jaoui, M., Flagan, R. C., and Seinfeld, J. H.: Evidence for organosulfates in secondary organic aerosol, Environ. Sci. Technol., 41, 517-527, 10.1021/es062081q, 2007.

Tammer, M.: G. Sokrates: Infrared and Raman characteristic group frequencies: tables and charts, Colloid and Polymer Science, 283, 235-235, 10.1007/s00396-004-1164-6, 2004.

Tang, M. J., Shiraiwa, M., Pöschl, U., Cox, R. A., and Kalberer, M.: Compilation and evaluation of gas phase diffusion coefficients of reactive trace gases in the atmosphere: Volume 2. Diffusivities of organic compounds, pressure-normalised mean free paths, and average Knudsen numbers for gas uptake calculations, Atmos. Chem. Phys., 15, 5585-5598, 10.5194/acp-15-5585-2015, 2015.

Wang, S., Liu, T., Jang, J., Abbatt, J. P. D., and Chan, A. W. H.: Heterogeneous interactions between SO2 and organic peroxides in submicron aerosol, Atmos. Chem. Phys., 21, 6647-6661, 10.5194/acp-21-6647-2021, 2021a.

Wang, Y., Zhao, Y., Wang, Y., Yu, J.-Z., Shao, J., Liu, P., Zhu, W., Cheng, Z., Li, Z., Yan, N., and Xiao, H.: Organosulfates in atmospheric aerosols in Shanghai, China: seasonal and interannual variability, origin, and formation mechanisms, Atmos. Chem. Phys., 21, 2959-2980, 10.5194/acp-21-2959-2021, 2021b.

Ye, J., Abbatt, J. P. D., and Chan, A. W. H.: Novel pathway of SO_2 oxidation in the atmosphere: reactions with monoterpene ozonolysis intermediates and secondary

organic aerosol, Atmos. Chem. Phys., 18, 5549-5565, 10.5194/acp-18-5549-2018, 2018.
Zhang, X., Cappa, C. D., Jathar, S. H., McVay, R. C., Ensber, J. J., Kleeman, M. J., and Seinfeld, J. H.: Influence of vapor wall loss in laboratory chambers on yields of secondary organic aerosol, P. Natl. Acad. Sci. USA, 111, 5802-5807, 2014.